Jinlin crater, Guangdong Province, China: Impact origin confirmed

Cite as: Matter Radiat. Extremes 11, 013001 (2026); doi: 10.1063/5.0301625 Submitted: 9 September 2025 • Accepted: 28 September 2025 • Published Online: 15 October 2025











Ming Chen,^{1,a)} Dayong Tan,¹ Wenge Yang,^{1,a)} Ho-Kwang Mao,^{1,2,a)} Xiande Xie,³ Feng Yin,¹ and Jinfu Shu¹



AFFILIATIONS

- ¹ Center for High Pressure Science and Technology Advanced Research, Shanghai 201203, China
- ²Shanghai Key Laboratory of MFree, Shanghai Advanced Research in Physical Sciences, Shanghai 201203, China
- ³Guangdong Academy of Sciences, Guangzhou 510070, China

Note: Paper published as part of the Special Topic on High Pressure Science 2026.

^{a)}Authors to whom correspondence should be addressed: ming.chen@hpstar.ac.cn; yangwg@hpstar.ac.cn; and maohk@hpstar.ac.cn

ABSTRACT

The newly identifie Jinlin crater in southern China lies on a hillside covered by a thick granite weathering crust. It appears as a slightly elliptical bowl-shaped depression with a diameter of 820-900 m. The structure is a tilted impact crater, showing a maximum rim height difference of about 200 m and an apparent depth of 90 m. The crater rim is composed mainly of granite weathered soil and a small amount of granite fragments, while the bottom of the crater is fille with the same mixture of granite weathered soil and granite fragments. Planar deformation features in quartz grains from the rock fragments of the crater provide decisive evidence for its impact origin. The impact event is inferred to have taken place during the Holocene.

Published under an exclusive license by AIP Publishing. https://doi.org/10.1063/5.0301625

Numerous impact craters have formed on Earth throughout its geological history. However, owing to tectonic activity and intense surface weathering, most ancient craters have been heavily eroded, deformed, or buried. To date, about 200 impact craters have been identifie worldwide. Within China's 9.6 × 10⁶ km² territory, only four impact craters have previously been reported, all of which are located in the northeastern region of the country.^{2,3} Southern China, by contrast, is characterized by tropical to subtropical monsoon climates, with abundant rainfall, high humidity, and elevated temperature conditions that promote intense chemical weathering.⁴ Granitic rocks are widespread across the region and have undergone extensive alternation.5 Here, we report the discovery of an impact crater formed on a granite mountain capped by a thick weathering crust in southern China [Fig. 1(a)].

The Jinlin crater is located in a low mountain and hilly region in the northwest of Guangdong Province, next to Jinlin Waterside-Village in Deqing County, Zhaoqing City [Fig. 1(b)]. It lies in the oasis zone of the Tropic of Cancer at 23°18′17″N and 111°48′49″E. The region has experienced intense tectonic and magmatic activities throughout much of geological history, with widespread exposure of Mesozoic granites. The Jinlin crater is situated within a large

Cretaceous granite batholith⁶ [Fig. 1(c)]. The upper part of this batholith has undergone strong chemical weathering, producing a granite weathering crust up to 80 m thick. This crust is stratifie from top to bottom into a soil layer, a granite debris layer, and a spherical weathering granite layer. Field observations from a nearby hill section indicate that the granite weathered soil exceeds 30 m in thickness, with no clear base exposed. These red to yellow granite weathered soils consist mainly of quartz and clay minerals, 5,8 with a bulk density of 1.06–1.43 g/cm³ that is substantially lower than the density of most rocks.8

Morphologically, the Jinlin crater appears as a bowl-shaped depression on the slope of a mountain with a highest elevation of 630 m [Fig. 1(a)]. The elevation at the foot of the mountain is 80 m. The crater is slightly elliptical, with a rim-to-rim diameter of 900 m in the northeast-southwest direction and 820 m in the northwest-southeast direction. It tilts southwestward by about 13°, consistent with the mountain slope. The apparent depth from the rim crest to the crater floo is about 90 m. The highest rim elevation on the uphill side reaches 355 m, while the lowest rim elevation downhill is 155 m. The elevation of the crater floo center lies at 160 m. The southern rim is breached by a vertical groove, forming a

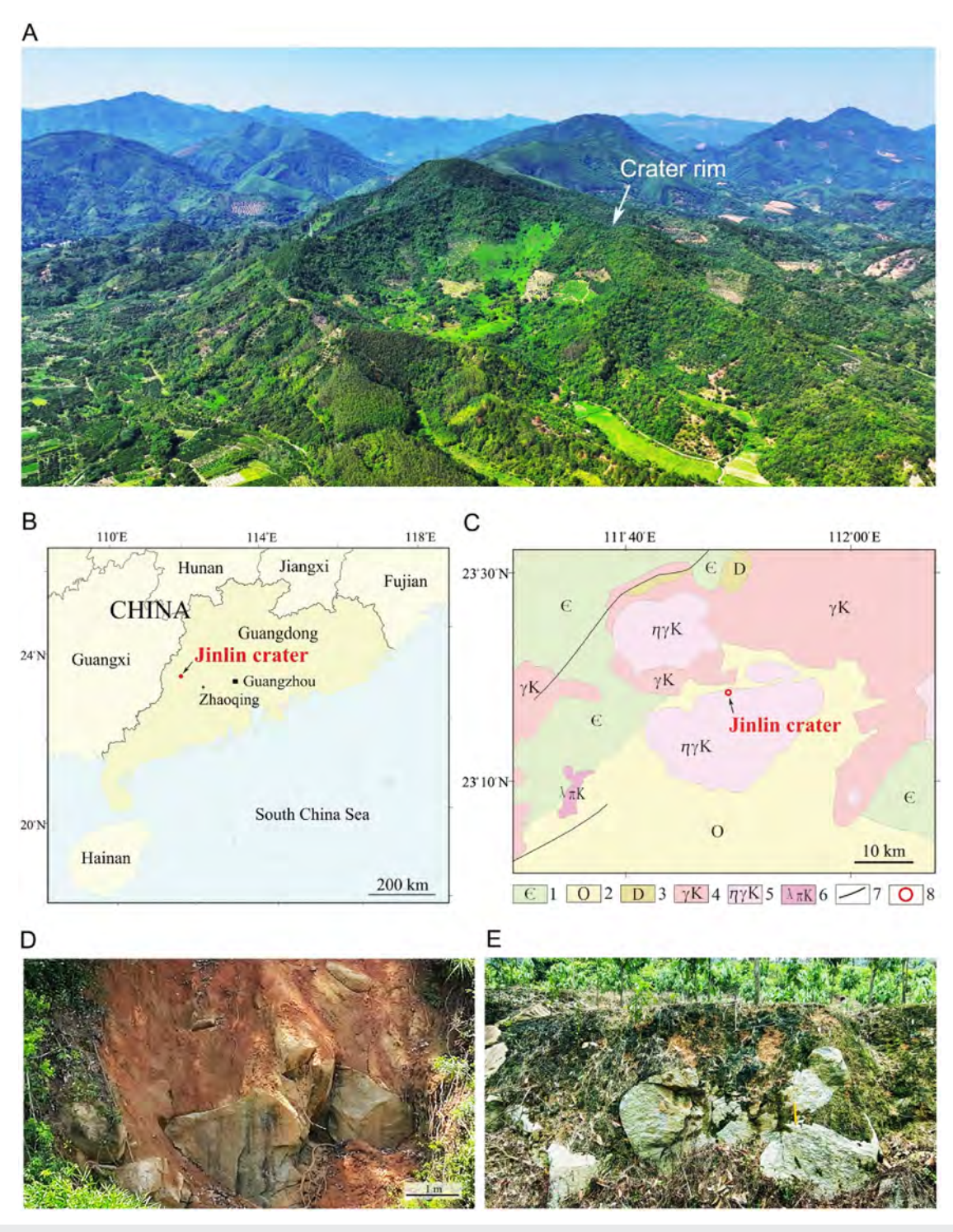


FIG. 1. The Jinlin crater. (a) Panoramic aerial drone image of the Jinlin crater, taken on May 12, 2025. (b) Location map showing the position of the Jinlin crater in northwestern Guangdong Province. The red dot marks the site of the crater. (c) Geological map of the Jinlin crater, modifie from Ref. 6: 1, Cambrian strata; 2, Ordovician strata (O); 3, Devonian strata (D); 4, Cretaceous granite (γK); 5, Cretaceous biotite monzonitic granite ($\eta \gamma K$); 6, Cretaceous granite porphyry ($\gamma \pi K$); 7. fault; 8. impact crater. (d) Geological section on the side slope of the V-shaped gap at the southern rim, showing mixed accumulation of red granite weathered soil and granite fragments. (e) Geological section at the crater floo , showing a mixed accumulation of granite weathered soil and granite fragments located at or near the surface are fresh. The orange ruler is 20 cm long.

V-shaped gap, which drains precipitation from the interior. Several large erosion gullies up to 10 m deep occur on the inner and outer walls of the crater rim, extending from crest to base.

The surface of the crater is covered with trees and grass. The crater rim is mostly well preserved, and is primarily composed

of granite weathered soil, with a small amount of rock fragments [Fig. 1(d)]. A significan concentration of rock fragments is exposed on the inner wall of the northern rim, while other sections of the rim contain relatively few rock fragments. The bottom of the crater is fille with a mixture of granite weathered soil and rock fragments

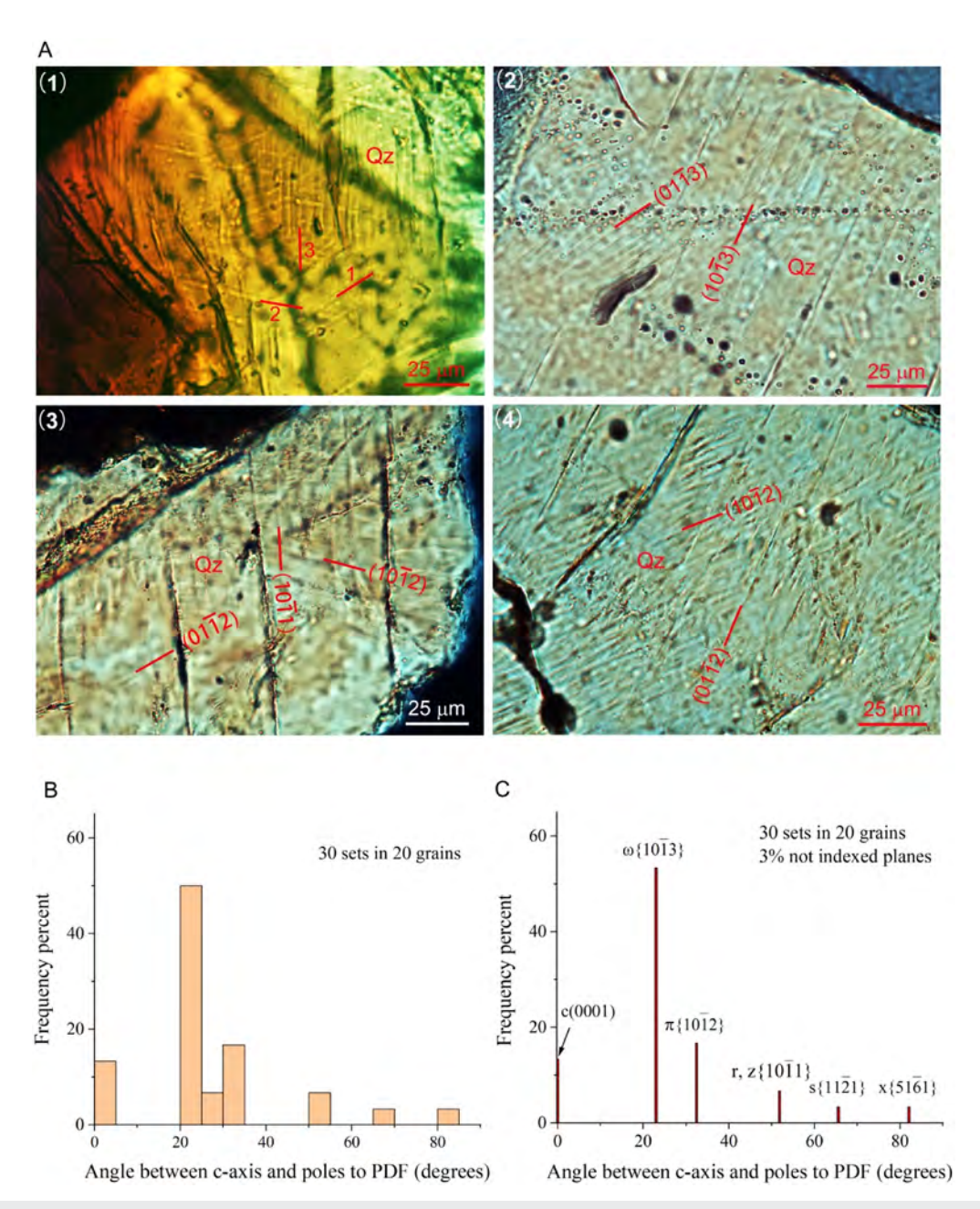


FIG. 2. Planar deformation features (PDFs) in quartz grains from the Jinlin crater. (a) Optical micrographs of PDFs in quartz (Qz) under cross-polarized light: (1) an unprocessed quartz clast showing three distinct sets of PDFs (labeled 1, 2, and 3 respectively); (2) thin-section micrograph with two sets of PDFs indexed as (1013) and (0113), respectively; (3) thin-section micrograph with three sets of PDFs indexed as (1011), (0112) and (1012), respectively; (4) thin-section micrograph with two sets of PDFs indexed as (01112) and (10112), respectively; (b) Histogram showing the frequency and angular distribution (5° bin size) of PDF planes relative to the c axis based on 30 sets of PDFs in 20 quartz grains. (c) Frequency distribution of crystallographically indexed PDF orientations from the same dataset.

[Fig. 1(e)]. These fragments, all of biotite monzonitic granite, can reach up to 4 m in size. Most granite fragments located at or near the surface show signs of weak chemical weathering or remain intact [Fig. 1(e)]. Only a small portion of granite fragments smaller than 30 cm, found beneath the topsoil and shielded from surface erosion, have undergone partial transformation into residual soil.

Shock-metamorphic effects in rocks and minerals from the Jinlin crater have been systematically investigated. Geological samples collected from the crater floo consist of granite debris and weathering-produced quartz, feldspar, biotite, and clay minerals. Planar deformation features (PDFs) have been identifie in quartz grains. Clearly define multiple sets of PDFs can be observed directly from some unprocessed quartz clasts [Fig. 2(a-1)]. To characterize the PDF features in quartz grains, 100 thin sections were prepared and examined using an optical petrographic microscope. A total of 53 quartz grains containing PDFs were identified These quartz grains exhibit one to three sets of PDFs [Figs. 2(a-2)–2(a-4)]. The individual PDF lamellae are ~1 μ m thick, with spacings between planes ranging from 2 to 8 μ m, consistent with the characteristics of standard PDFs. 9,10

Crystallographic orientations of 30 PDF sets in 20 quartz grains were further analyzed using a four-axis universal stage and a stere-ographic projection aided by a Wulff net. ⁹⁻¹¹ The most frequently observed PDF orientations correspond to Miller indices $\omega\{10\overline{1}3\}$ (53.3%) and $\pi\{10\overline{1}2\}$ (16.7%) [Figs. 2(b) and 2(c)]. Other observed orientations include c(0001), r, z{10\$\overline{1}1\$}, and \xi{11\$\overline{2}2\$} [Figs. 2(b) and 2(c)]. These PDFs in quartz are diagnostic of shock metamorphism, forming only under shock pressures ranging from 5 to 30 GPa. ^{9,12} Their presence provides definitive vidence for an impact origin of the Jinlin crater.

The hypervelocity impact of an extraterrestrial object on Earth's surface generates extreme compression, fragmentation, excavation, and ejection of target rocks, ultimately resulting in crater formation. On the basis of established scaling relationships between impactor size and crater diameter, the object responsible for forming the Jinlin crater is estimated to have been about 30 m in diameter. Giving a typical terrestrial impact velocity of 15–25 km/s, the impactor would have penetrated to a depth of one to two times its own diameter, excavating and ejecting target materials from within that range. Consequently, the maximum depth of ejected materials at the Jinlin crater could be about 60 m, coinciding with the interface between the granite weathering crust and the underlying granite bedrock, located at a depth of ~60–80 m in this region.

During the Jinlin impact event, the asteroid struck a granite hillside covered by a thick weathering crust. Large amounts of granite weathered soil were ejected and deposited around the crater rim. The distribution of a large amount of granite fragments on the inner wall of the northern rim suggests that the weathering crust was thinner on the uphill (northern) side than on the downhill (southern) side. In the north, the impact partially excavated the deeper granite bedrock, which was then ejected toward the rim. By contrast, the southern portion of the crater contains a thicker weathering crust, and the ejected materials from this area consist primarily of granite weathered soil.

Low-density and high-porosity weathered materials can act as a momentum trap for an impactor, reducing the ejection velocity of the target materials.¹⁵ As a result, owing to the thick weathering layer, the excavated rock fragments deep in the crater could not be

ejected to the rim position in large quantities. Instead, some of these fragments either fell back into the crater or slumped from the walls, accumulating on the bottom of the crater.

The crater rim, primarily composed of loose soil, is geologically unstable and highly vulnerable to erosion. Deqing Country receives more than 1500 mm of rainfall annually, ¹⁶ and heavy precipitation often accelerates soil erosion. In this region, the collapse of granite weathered soil on mountain slopes is a common occurrence during periods of intense rainfall. ^{7,8} The development of large erosion gullies along the rim of Jinlin crater is closely linked to such soil collapse triggered by rainwater erosion. The V-shaped gap on the southern rim also reflect the effects of water erosion originating from inside the crater. Under conditions of strong chemical weathering and persistent rainfall erosion, the remarkably well-preserved state of the Jinlin crater suggests that it represents a relatively young impact structure that has not been severely eroded.

The chemical weathering rate of granite in the low mountain and hilly region of northern Guangdong Province has been measured at 0.038 mm/year. Since the Deqing Country shares the same geographical environment, the granite weathering rate there is expected to be comparable. At this rate, a granite fragment smaller than 30 cm within the Jinlin crater would be completely transformed into residual soil in less than 10 000 years. However, the granite fragments of this size in the crater surface have only undergone incomplete soil transformation. This suggest that the impact event most likely occurred during the early to middle Holocene. Further studies are required to determine the precise age of the crater. The known Holocene impact craters range from 14 to 300 m in diameter, and the discovery of Jinlin Crater may therefore indicate a relatively large-scale impact event within the Holocene.

Southern China covers about one-quarter of the nation's land area. The Jinlin crater is the firs confirme impact structure in this region. Its discovery provides an important reference point for future studies of impact sites across southern China.

H. Mao acknowledges financia support from Shanghai Key Laboratory Novel Extreme Condition Materials, China (Grant No. 22dz2260800) and the Shanghai Science and Technology Committee, China (Grant No. 22JC1410300).

REFERENCES

- ¹T. Kenkmann, "The terrestrial impact crater record: A statistical analysis of morphologies, structures, ages, lithologies, and more," Meteorit. Planet. Sci. 56, 1024–1070 (2021).
- ²M. Chen, C. Koeberl, W. Xiao, X. Xie, and D. Tan, "Planar deformation features in quartz from impact-produced polymict breccia of the Xiuyan crater, China," Meteorit. Planet. Sci. **46**, 729–736 (2011).
- ³F. Yin, M. Chen, W. Yang, and H.-k. Mao, "Discovery of the Hailin impact crater in northeast China," Matter Radiat. Extremes 10, 013001 (2025).
- ⁴F. Wu, Z. Jiang, and S. Zhou, "Review of geological survey of the weathered crust at home and abroad," Geol. Sur. China 5, 41–47 (2018).
- ⁵Z. Wu and J. Wang, "Relationship between slope disintegration and rocksoil characteristics of granite weathering mantle in South China," J. Soil Water Conserv. 14, 31–35 (2000).
- ⁶H. Geng, X. Xu, S. Y. O'Reilly, M. Zhao, and T. Sun, "Cretaceous volcanic-intrusive magmatism in western Guangdong and its geological significance, Sci. China Ser. D **49**, 696–713 (2006).

- ⁷J. Xie, "Management and prevention measures of collapsed hills in Deqing Country," Subtrop. Soil Water Conserv. 18, 52–54 (2006).
- ⁸R. Zhuo, X. Liu, and M. Yue, "Physical and chemical properties of Benggang soils and their interior differentiation," Bull. Soil Water Conserv. **42**, 38–45 (2022).
- ⁹D. Stöffle and F. Langenhorst, "Shock metamorphism of quartz in nature and experiment: I. Basic observation and theory," Meteoritics **29**, 155–181 (1994).
- ¹⁰F. Langenhorst, "Shock metamorphism of some minerals: Basic introduction and microstructural observations," Bull. Czech Geol. Surv. 77, 265–282 (2002).
- ¹¹L. Ferrière, J. R. Morrow, T. Amgaa, and C. Koeberl, "Systematic study of universal-stage measurements of planar deformation features in shocked quartz: Implications for statistical significanc and representation of results," Meteorit. Planet. Sci. 44, 925–940 (2009).
- ¹² R. A. F. Grieve, F. Langenhorst, and D. Stöffler "Shock metamorphism of quartz in nature and experiment: II. Significanc in geoscience," Meteorit. Planet. Sci. 31, 6–35 (1996).
- ¹³B. M. French, Trace of Catastrophe: A Handbook of Shock-Metamorphic Effects in Terrestrial Meteorite Impact, LPI Contribution 954 (Lunar and Planetary Institute, Houston, TX, 1998).
- ¹⁴H. J. Melosh and R. A. Beyer, "Computing projectile size from crater diameter" (1999); https://pirlwww.lpl.arizona.edu/~rbeyer/crater_p.html.
- ¹⁵K. R. Housen and K. A. Holsapple, "Impact cratering on porous asteroids," Icarus 163, 102–119 (2003).
- ¹⁶S. Zhang, "Flood and waterlogging disasters in Deqing Country and their countermeasures," Pear River 1, 29–31 (1996).
- ¹⁷H. Yang and S. Zhou, "Application of uranium disequilibrium in the study of the weathering rate of the granite in northern Guangdong," J. South. China Normal Univ. Nat. Sci. Ed. **51**, 84–91 (2019).